Dynamic Mechanical Properties of Typical CFRP Laminate Under High-impact Compressive Loads

W Wu[1], L Liu[2], Y Chu[1], A Pi[1]*

1. State Key Laboratory of Explosion Science and Technology, Beijing Institute of Technology, Beijing, China
2. Southern Sichuan Machinery, Luzhou, China

ABSTRACT

Because of its outstanding mechanical properties, carbon fiber reinforced plastic (CFRP) is widely used in structures bearing high-impact loads. In this study, based on the bridging model, the dynamic constitutive equations and yield criteria concerning the strain rate effect of composite material are used to analyze the optimal design and compressive strength of a CFRP laminate under high-impact compressive loads. The mechanical properties of laminates under different strain rates were calculated and compared with experimental results to verify the viability of improving the bridging model, where our theoretical results agreed with them. Structural design schemes based on this were analyzed and a ply scheme satisfying our requirements selected. Using this scheme, samples were manufactured and subjected to quasi-static and medium strain rate compressive tests, and the results agreed with theoretical calculations. This study can help design optimal CFRP structures for penetrator case under high-impact compressive loads and predict their properties.

1. INTRODUCTION

Carbon fiber reinforced plastic (CFRP) is a composite material with carbon fiber as reinforcing material and synthetic resin as matrix. Because of such properties as low density, high specific strength, high specific modulus, high toughness, corrosion resistance, and high impact resistance, it is widely used in aerospace, aviation, military, and other fields.

The mechanical properties and failure mechanism of composite materials under high-impact loads are very complex, and the dynamical mechanical properties of composite materials, such as carbon fiber reinforced composite materials, are significantly influenced by the strain rate. The dynamic stress–strain response of [±45°/0°/90°] graphite fiber epoxy composite was studied by Thiruppukuzhi [1], who concluded that, for the same sample, the greater the strain rate, the greater the strength. Jadhav et al. [2] studied the dynamic compressive properties of a graphite fiber epoxy laminate with different ply angles, where the results showed that although fiber is insensitive to strain rate, composite materials feature a strong strain rate effect such that with decreasing fiber angle, the strain rate effect gradually increases. The strain hardening effect of CFRP was observed by Ochola et al. [3], where the failure mode of the material under a low strain rate was shear failure, and failure

*Corresponding Author: aiguo_pi@bit.edu.cn

phenomena such as fiber matrix debonding, delamination, and matrix destruction were observed under a high strain rate. A study by Naik et al. [4] showed that the compressive modulus and strength of CFRP had clear strain rate strengthening effect under a high strain rate. Kara et al. [5] found that the compressive stress–strain relationship of composites was sensitive to strain rate along all the three directions, and the strain rate effect when loading in-plane was more obvious than when loading along the direction of thickness. The mechanical response of composites under high-impact load can be generally divided into macro- and micro-mechanical models. The macro model can only analyze the overall structure of the composite, and cannot analyze the properties of the reinforcement and matrix, whereas the micro-mechanical model can obtain the macro-mechanical properties by analyzing microscopic parameters. The mixed method model [6], the Chamis formula proposed by Hopkins and Chamis [7-8], and the Hill–Hashin–Christensen–Lo model proposed by Hill and Hashin [9-12] are commonly used micro-mechanical models. The bridging model proposed by Huang Zhengming [13-14] is more accurate, and can be used to calculate laminate strength. However, the bridging model is not suitable for studying the dynamical mechanical properties of laminate structures. Based on the bridging model, Zhang Huashan [15] assumed that the fiber, matrix, and composite material were rate independent, and studied the low-velocity impact load-carrying capacity of composite laminate by ABAQUS. The micro-mechanical finite element model was used to calculate the mechanical properties of different laminates under impact loads, but the strain rate effect of the laminate structure could not be represented. Mahmood et al. [16-17] adopted the Goldberg rate-dependent constitutive equation to describe the nonlinear mechanical properties of glass fiber reinforced plastic (GFRP), and combined this with the bridging model to study the strain rate dependence of GFRP. Few studies based on bridging model have explored the strain rate effect of CFRP materials [18].

Grudza et al. [19] studied the properties of a composite structure used for penetrator case. In order to apply CFRP structures into potential usage like penetrator case, the dynamic properties of CFRP were researched. In this study, based on the above research, the rate dependence of CFRP is considered, and the dynamic constitutive equations and yield criterion concerning the strain rate effect are used to improve the bridging model. Then the improved model is embedded into program. Combined with experimental data from the literature, the improved bridging model is verified. Optimization design and compressive strength analyses were conducted on the CFRP composite laminate under high-impact loads.

2. IMPROVEMENT AND VERIFICATION OF DYNAMIC STRENGTH THEORY FOR CFRP LAMINATE STRUCTURE BASED ON BRIDGING MODEL

The bridging model is a kind of typical composite micro-mechanics model. This model combines fiber stress with matrix stress using a non-singular matrix. Thus, the fiber stress and matrix stress can be determined by the overall stress, and the micro-mechanical properties of the material can be expressed clearly. The bridging model can be used to analyze elastic problems in fiber reinforced composites and extended to calculate such non-elastic properties as the ultimate strength of the composite material.

Comparing the dynamic mechanical response of composite laminate with its static mechanical response, the main differences are the different constitutive relations and failure criteria. To obtain a model of the strength of composite laminate under a dynamic in-plane load, based on the bridging model, the dynamic constitutive

2.1. Dynamic Constitutive Relation

For the bridging model, the constitutive equations of fiber, matrix, and the composite material are [6]:

$$\{\sigma_i\} = V_f \{\sigma_i^f\} + V_m \{\sigma_i^m\} \tag{1}$$

$$\{\varepsilon_i\} = V_f \{\varepsilon_i^f\} + V_m \{\varepsilon_i^m\} \tag{2}$$

$$\{\varepsilon_i^f\} = [S_{ij}^f]\{\sigma_j^f\} \tag{3}$$

$$\{\varepsilon_i^m\} = [S_{ij}^m]\{\sigma_j^m\} \tag{4}$$

$$\{\varepsilon_i\} = [S_{ij}]\{\sigma_j\} \tag{5}$$

Where $[S_{ij}^f]$, $[S_{ij}^m]$, and $[S_{ij}]$ are, respectively, the flexibility matrix of fiber, the matrix, and the composite material, $\{\sigma_i^f\}$, $\{\sigma_i^m\}$, and $\{\sigma_i\}$ are the stress tensors of fiber, matrix, and composite material, respectively, $\{\varepsilon_i^f\}$, $\{\varepsilon_i^m\}$, and $\{\varepsilon_i\}$ are the strain tensor of fiber, matrix, and composite material, respectively, and Vf and Vm are the volume fraction of fiber and matrix, respectively.

Based on the assumption of an ideal bond, a non-singular matrix can be used to relate the fiber and the matrix as long as the composite does not fail:

$$\{\sigma_i^m\} = [A_{ij}]\{\sigma_j^f\} \tag{6}$$

Where $[A_{ij}]$ is the bridging matrix eponymous of the bridge model.

For composite materials subjected to impact loads, the elastic modulus, failure strain, and strength of the materials exhibit a certain degree of the strain rate hardening phenomenon. Therefore, the dependence of the strain rate should be considered for the composite material. A number of researches have recently shown that the mechanical properties of composite materials are closely related to the those of component materials. Chen et al. [20] and Gilat et al. [21] found that the exposy resin matrix has a clear strain rate hardening effect. The experimental study conducted by Han Xiaoping et al. [22] showed

that the resin matrix was viscoelastic under a high strain rate. The study by Zhou and Xia [23] indicated that the elastic modulus and tensile strength of T300 carbon fiber were independent of strain rate. In summary, we make the following assumptions: First, fiber is a homogeneous, transversely isotropic material assumed to be perfectly elastic for the dynamic constitutive model of composite materials. Second, we ignore the influence of the strain rate effect of fiber on the mechanical properties of composite laminate. Third, the matrix material is seen as a homogeneous isotropic material that exhibits some viscoelastic properties during the impact process, which is the main cause of the strain rate effect of the composite material. Therefore, the effect of strain rate on the mechanical properties of the matrix is considered.

For the resin matrix component, the dynamic damage constitutive model of fiber reinforced composite materials was studied by Karim [24]. The stress–strain relationship of the matrix under a constant strain rate was presented as:

$$\sigma_m = E_m\varepsilon_m + E_1\theta_{e1}\dot{\varepsilon}\left(1-e^{-\frac{\varepsilon_m}{\dot{\varepsilon}\theta_{e1}}}\right)+E_2\theta_{e2}\dot{\varepsilon}\left(1-e^{-\frac{\varepsilon_m}{\dot{\varepsilon}\theta_{e2}}}\right) \tag{7}$$

To connect with the model and simplify the calculation, the Cowper and Symonds model [25] is used to describe the rate-dependent constitutive model of the matrix and composite materials. Equations (1), (2), and (3) are used as are, whereas Equations (4) and (5) are modified as (8) and (9), respectively:

$$\sigma_m = E_m\left(1+\left(\frac{\dot{\varepsilon}}{c}\right)^{\frac{1}{p}}\right)\varepsilon_m \tag{8}$$

$$\text{X direction: } \sigma = E\left(1+\left(\frac{\dot{\varepsilon}}{484.67}\right)^{\frac{1}{0.4942}}\right)\varepsilon$$

$$\text{Y direction: } \sigma = E\left(1-\left(\frac{\dot{\varepsilon}}{1856}\right)^{\frac{1}{0.5094}}\right)\varepsilon \tag{9}$$

Where Equation (9) is obtained by fitting the experimental data of the CFRP composite material while the parameters in Equation (8) are obtained by fitting the stress–strain relation in Equation (7). The matrix used in this paper is composed of homemade toughened epoxy resin, the properties of which are similar to those of the 3501-6 epoxy resin matrix. Without loss of generality, the parameters of the 3501-6 epoxy matrix in reference [24] were used.

Table 1. The parameters of the matrix material in reference [24]

Parameter	**Value**
Modulus, E_m [GPa]	2.31
Viscoelastic constant modulus, E_1 [GPa]	0.971
First characteristic relaxation time for normal stresses,θ_{e1} [ms]	0.041
Viscoelastic constant modulus, E_2 [GPa]	0.104
Second characteristic relaxation time for normal stresses, θ_{e2} [ms]	121000

Fitting parameters c = 1772 and p = 0.2442 were obtained, and the fitting results are shown in Figure 1.

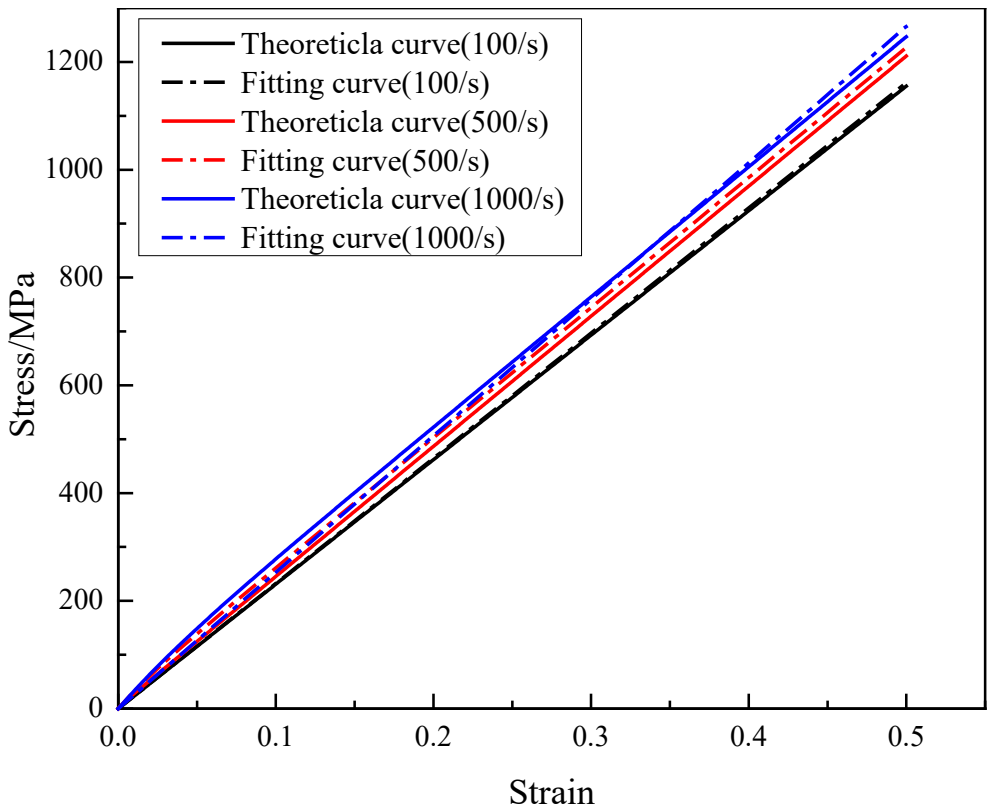

Figure 1. Comparison between the theoretical and experimental fitting of the stress-strain curve of the matrix.

2.2 Dynamic Failure Criteria

The failure criterion used in quasi static action is from the maximum tensile stress theory, and the damage to composite materials is determined by detecting the failure of the fiber and matrix. When any one of the following four equations is satisfied, the material is deemed to have failed [6]:

$$\frac{\sigma_{11}^f+\sigma_{22}^f}{2}+\frac{1}{2}\sqrt{\left(\sigma_{11}^f-\sigma_{22}^f\right)^2+4\left(\sigma_{12}^f\right)^2}\geq\sigma_u^f, \tag{10}$$

$$\frac{\sigma_{11}^f+\sigma_{22}^f}{2}-\frac{1}{2}\sqrt{\left(\sigma_{11}^f-\sigma_{22}^f\right)^2+4\left(\sigma_{12}^f\right)^2}\leq-\sigma_{u,c}^f, \tag{11}$$

$$\frac{\sigma_{11}^m+\sigma_{22}^m}{2}+\frac{1}{2}\sqrt{\left(\sigma_{11}^m-\sigma_{22}^m\right)^2+4\left(\sigma_{12}^m\right)^2}\geq\sigma_u^m, \tag{12}$$

$$\frac{\sigma_{11}^m+\sigma_{22}^m}{2}-\frac{1}{2}\sqrt{\left(\sigma_{11}^m-\sigma_{22}^m\right)^2+4\left(\sigma_{12}^m\right)^2}\leq-\sigma_{u,c}^m. \tag{13}$$

Where σ_{11}^f, σ_{22}^f, and σ_{12}^f, and σ_{11}^m, σ_{22}^m, and σ_{12}^m are the components of the principal stress of the fiber and matrix, respectively, σ_u^f, $\sigma_{u,c}^f$ and σ_u^m, $\sigma_{u,c}^m$ are their tensile and compressive strength, respectively.

The failure mode and main failure mechanism of composite materials are nearly identical on the condition of dynamic and quasi-static loads. The bridging model determines the failure of the composite material through fiber breakage and matrix cracking. Interlaminar delamination, and fiber matrix debonding are not considered. However, the strain rate has a certain effect on the strength parameters of the material. Therefore, the same failure criterion can be used in dynamic strength analysis, but the strength parameters need to be modified in consideration of the strain rate.

The relationship between the strength parameters and strain rate of the composite materials can be expressed in Cowper and Symonds form:

$$S=S_0\left(1+\left(\frac{\dot{\varepsilon}}{c}\right)^{\frac{1}{p}}\right) \tag{14}$$

Where S is the strength under the given strain rate, S_0 is the static strength parameter, and c and p are the strain rate correction factors for the corresponding strength. The strain rate effect of the matrix can be described by selecting different strain rate correction parameters according to matrix material.

On the basis of the theory above, the bridging model is adaptively improved to calculate the mechanical response and predict the dynamic strength of the laminate subjected to dynamic load.

2.3 Verification and Validation of Theoretical Calculation Program of Dynamic Strength of CFRP Laminate Structure Based on Bridging Model

The verification and validation (V&V) of the theoretical model based on the relevant experimental results is important. Moura [25] gave the stress–strain curve of $[0]_{32}$ unidirectional laminate under at a compression angle of 90° under conditions of quasi-static loads and strain rates of 82 /s, 163 /s, and 817 /s. Experimental data for the compressive stress–strain of CFRP $[0/90/\pm45]_{2s}$ laminate when the strain rates were 0.0001 /s, 0.07 /s, and 400/s were provided by Guedes and Moura et al. [27]. These two groups of experimental data were selected to verify the theoretical model. For the different matrices in the two experiments, modified coefficients for the strength–strain rate of the matrix were obtained by fitting the experimental data. For the matrix used by Moura et al., the modified coefficients were $c = 5109$ and $p = 1.873$, and for the matrix used by Guedes, the coefficients were $c = 3.831$ and $p = 1.761$. Based on the improved theoretical model, with the help of a computer, the theoretical stress–strain curves were calculated and compared with the experimental data. The results are shown in Figure 2.

Figure 2 shows that the dynamic strength calculation program can accurately estimate the strength of the laminates. The configuration of the stress–strain curves was roughly consistent, and the improved bridging model can thus be used to study the mechanical properties of the CFRP laminate structure under dynamic compression. The difference shown in Figure 2 was reflected in the phenomenon whereby the theoretically calculated strength was slightly higher than the test results, the predicted failure strain deviated, and there was no stress drop process. Under a dynamic load, the main reason for the higher predicted strength was that the bridging model did not considered layered stress, and considered only fiber breakage and the failure mode of the matrix. Another reason for the higher strength is that the stress concentration factor [18] was not considered. The strength of the matrix after adding the fiber was not equal to its original strength, and this can be corrected by the stress concentration factor. The correction of the delamination and the strength of the matrix in the theoretical calculation was not considered, so that the theoretical strength was slightly higher than the test results. The error in the failure strain was related to initial imperfections in and the random dispersion of the test samples during the machining process. There was no stress drop process for the theoretical calculation because the selected failure criterion determined the failure by fiber and matrix strength. When stress in the fiber or the matrix reached failure strength, the layer was identified as having been destroyed, because of which there was no drop in stress. According to the above analysis, the form of rate dependence selected for composite strength, namely the Cowper and Symonds power function, can accurately show the strain rate hardening effect of CFRP composite materials, and the improved theoretical model can be used to calculate the dynamic strength of CFRP materials.

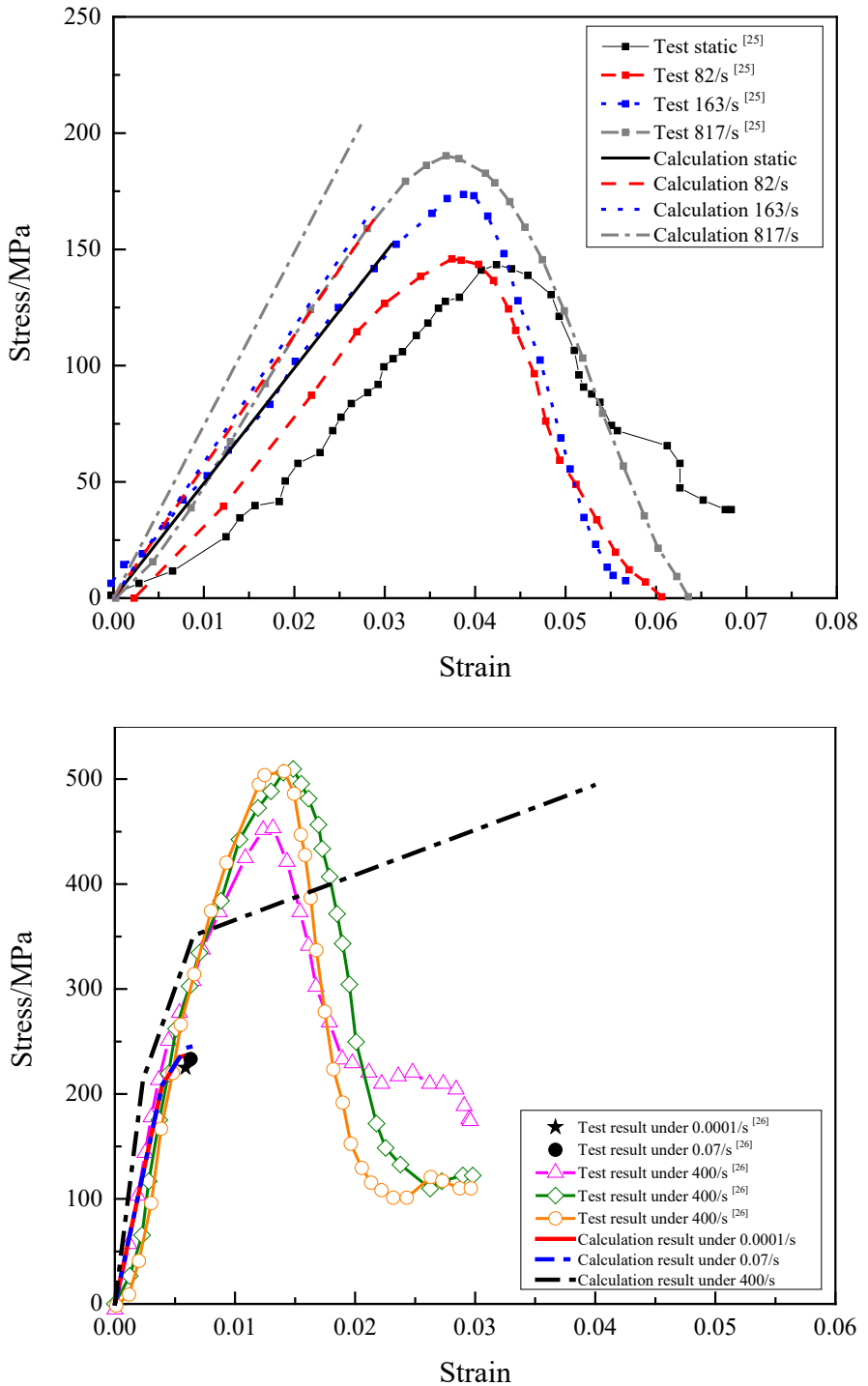

Figure 2. The theoretical and experimental stress–strain curves of two laminates under in-plane dynamic compression.

3. ANALYSIS OF STRUCTURAL DESIGN AND MECHANICAL PROPERTIES OF CFRP LAMINATE WITH HIGH-IMPACT LOAD

The appropriate selection of a ply sequence is an important technical approach to optimize the mechanical properties of CFRP laminated structures. In this section, several typical ways of designing ply sequence are detailed. The strength of these laminates under in-plane compression along the X and Y directions when the strain rate was 750 /s was calculated by using the above model. The ply sequence with the best mechanical properties was selected as optimal by a comparison of the laminates, where laminate samples were manufactured and subjected to quasi-static and medium strain rate compression. The prepared samples were composed of T700 carbon fiber produced by Toray and homemade modified epoxy resin. The parameters of the fiber and matrix are shown in Table 2.

Table 2. Parameters of materials of fiber and matrix

Parameters	**Fiber**	**Matrix**
Tensile Modulus E_T [GPa]	230	3.5
Tensile Strength σ_u [MPa]	4900	98
Compressive Modulus E_C [GPa]	15	3.5
Compressive Strength $\sigma_{u,c}$ [MPa]	1500	100
Density ρ [g/cm^3]	1.8	1.26

3.1 Theoretical Calculation of CFRP Laminate Structure with Six Modes of Ply Sequence

The six ply sequences used for theoretical calculations are shown in Table 3. The numbers of plies was 49 in all cases.

Table 3. Six lay-up conditions for laminate

Number	**Ply Sequence**
LAM-01	$[(0/90/0_3/\pm45/0_3)_4/0/90/0_3/\pm45/0_2]$
LAM-02	$[(0/90/0_3/\pm45/0_3)_3/0/90/0_3/\pm45/0/90/\pm45/(0/90)_4]$
LAM-03	$[(0/90/\pm20/0_4)_5/(0/90)2/\pm_20/0_3]$
LAM-04	$[(\pm45/(\pm30)_2)_6/\pm45/\pm30/(0/90)_4/0]$
LAM-05	$[(\pm45/(\pm30)_2/0_5/90/(\pm30)_2)_2/0/(\pm45/0/90)_4]$
LAM-06	$[(\pm30/(\pm15)_2/0_5/90/\pm15/(0/90)_3)_2/\pm30/(\pm15)_2/0_3]$

On the basis of the experimental data for the CFRP composite material, the modified coefficients of the strength–strain rate of the matrix were obtained by fitting, Along the X direction, the strain rate coefficients were c = 134 and p = 0.9007, and were c = 1131 and p = 0.5819 along the Y direction. The results are shown in Figures 3 and 4.

Figures 3 and 4 show that of laminates subjected to in-plane tension, LAM-03 and LAM-01 had higher strength along the X direction, and the strength of LAM-02 and LAM-03 was higher than that of the others along the Y direction. Along both directions, LAM-04 and LAM-05 had lower strength. For laminates subjected to in-plane compression, along the X direction, LAM-02 and LAM-01 had a higher strength, whereas LAM-03 and LAM-04 had relatively low strength. Along the Y direction, the strength of LAM-02 and LAM-05 was higher than that of the others, whereas the strength of LAM-03 and LAM-04 was low. We can conclude that of the six ply sequences, by considering the strength along the X and Y

direction under in-plane tension and compression, LAM-02 exhibited the best mechanical properties. Therefore, in the subsequent experiments, the LAM-02 ply sequence was selected to prepare samples and test quasi-static and medium strain rates.

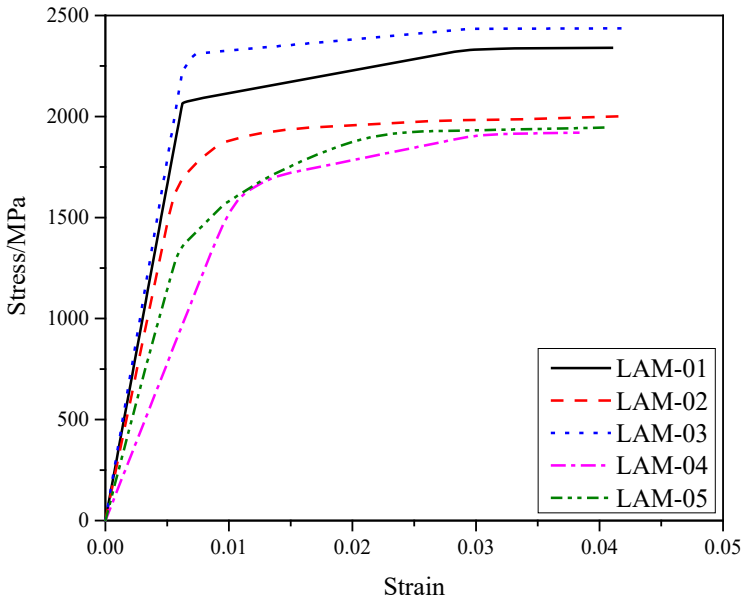

(a) X direction

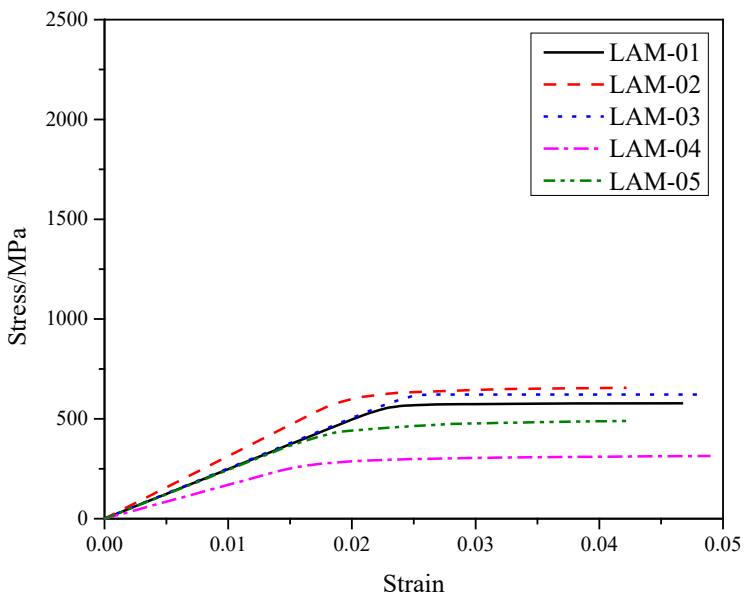

(b) Y direction

Figure 3. Stress–strain curve of different lay-up laminates with in-plane tension along the X and Y directions.

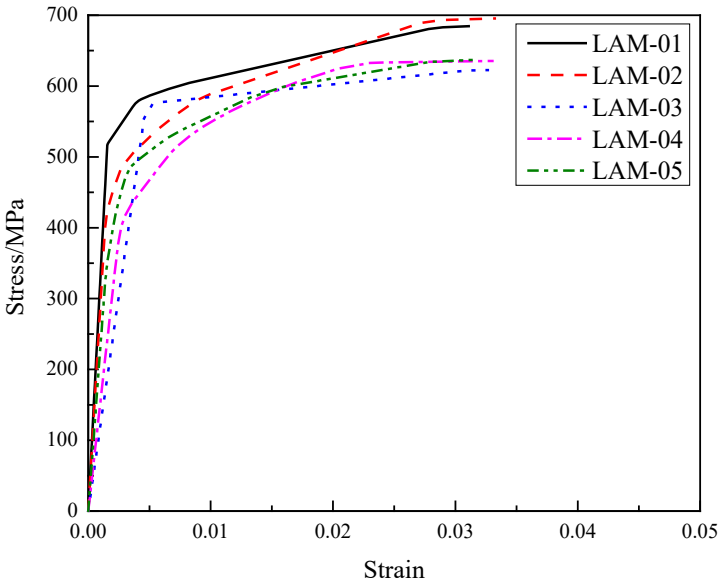

(a) X direction

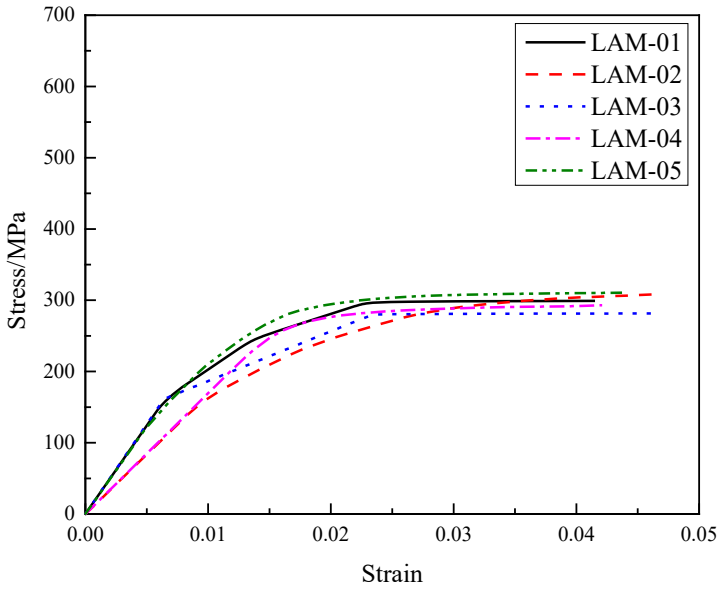

(b) Y direction

Figure 4. Stress–strain curve of lay-up laminates with in-plane compression along the X and Y directions.

3.2 Experiment on Mechanical Properties of LAM-02 Laminate

The quasi-static compression test was performed on the INSTRON electronic universal testing machine. On the basis of the predicted failure strength of the sample, the default maximum load was 2 KN.

In the test, the sample size of LAM-02 was 9 × 9 × 8 mm and the strain rate was 0.001 /s. One loading test was performed on the specimen until the material was destroyed. The stress and strain data of the samples were processed using Origin software, and their stress–strain curves were obtained by theoretical calculation and compared with experimental data. Some fabrication errors, such as perpendicularity, levelness, and surface finish of sample cross-section, affected the test results. As shown in Figure 5, nonlinear characteristics were briefly observed in the beginning owing to the form and position errors in the material during processing and the manufacturing process. It is evident from the stress–strain curve of the test that before the strain was 0.008~0.01, there was an obvious nonlinear characteristic in the test curve, i.e., a deformation error $\delta \approx \varepsilon \cdot L$ = 0.008 × 9 mm = 0.072 mm led to the nonlinear characteristics.

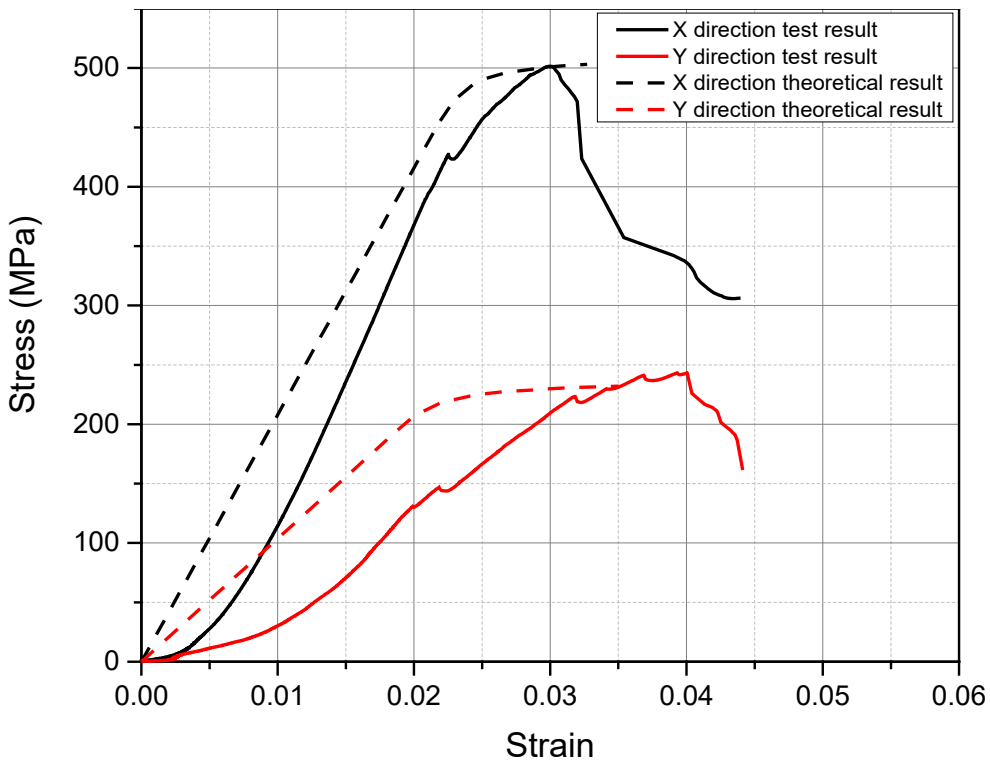

Figure 5. Quasi-static compressive stress–strain curve of LAM-02.

From the experimental data in Figure 5, it is clear that such parameters as compressive failure strength showed obvious anisotropic characteristics. The compressive stress–strain curve along each direction was also significantly different. Along the X direction, the compressive strength was 501 MPa, and strain was only 0.03, whereas along the Y direction,

the compressive strength was only 243 MPa, and the corresponding strain was 0.04. The theoretical value for strength was slightly higher than the experimental value, which is consistent with past analysis. Both the yield limit and the compressive strength along the X and Y directions were more accurate, error in the failure strain value was larger, and error along the Y direction was larger than that along the X direction. The error was mainly due to two aspects: on the one hand, in the theoretical calculations, owing to the random dispersion in processing, the input parameters of the matrix were difficult to determine exactly; on the other hand, the selection of sample size and the existence of fabrication error during the manufacturing process had an effect on the experimental results, which led to errors.

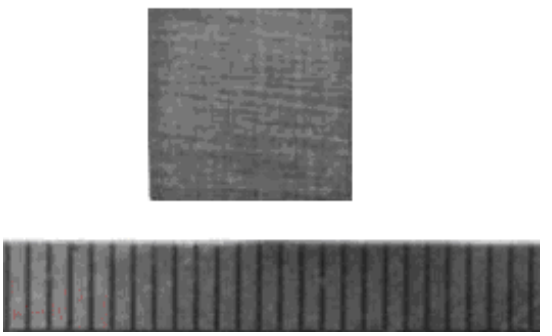

(a) Morphology of original sample

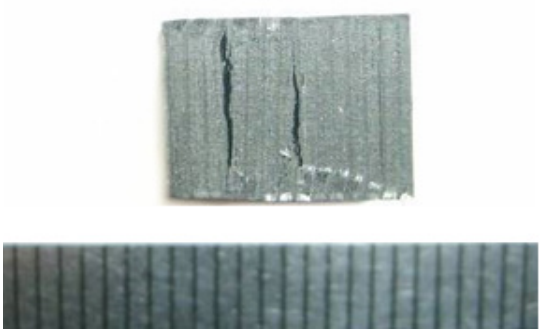

(b) Failure mode along the X direction

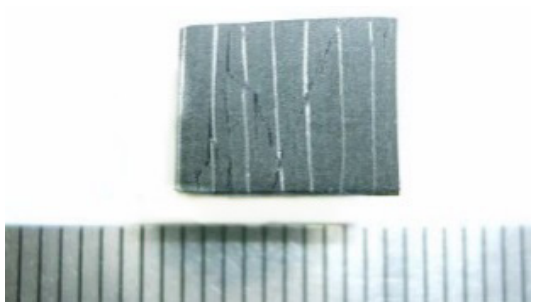

(c) Failure mode along Y direction

Figure 6. The failure mode of CFRP along the X- and Y directions under quasi-static compression when the strain rate was 0.001 /s.

Along the X and Y directions, except for the short nonlinear lines at the beginning of the stress–strain curves, all lines showed obvious linear features owing to the combined effect of the carbon fiber and the matrix. In addition to these, the properties of the material were determined by the initial micro-buckling of the fiber and the strength of the bond between layers. As shown in Figure 6(b), the main failure mode along the X direction was interlaminar fracture. Two cracks parallel to the ply are shown in pictures of the recycling specimen, clearly produced by interlaminar fracture. This phenomenon indicates that interlaminar strength is an important aspect in restricting the strength of CFRP. Studies by Hosur [26] and Moura et al. [28-29] have also shown that the strength of the laminate CFRP was closely related to the delamination phenomenon and interlaminar strength. Figure 6(c) shows that except for a crack at 90° with respect to the loading direction, the recycling specimen also had a large number of small cracks, which indicates that the failure mode included the shear of the matrix and interlaminar damage. The generation of micro-cracks is related to the non-uniformity of stress during the curing process of the specimens, the difference in degree of interlaminar bonding, the difference in the degree of the initial micro-buckling of the fiber, and other factors.

3.3 Experiment on Mechanical Properties under Dynamic Compression

To study the mechanical properties of the CFRP laminated structure under dynamic compression, the stress–strain curves of the CFRP material along the X and Y directions were obtained by using the split Hopkinson pressure bar test system (SHPB), and the strain rate dependence of the dynamical mechanical properties and failure modes were analyzed. A comparison between the experimental compressive stress–strain curve of the LAM-02 CFRP composite laminate along the X and Y directions and the results of theoretical calculations is shown in Figure 7.

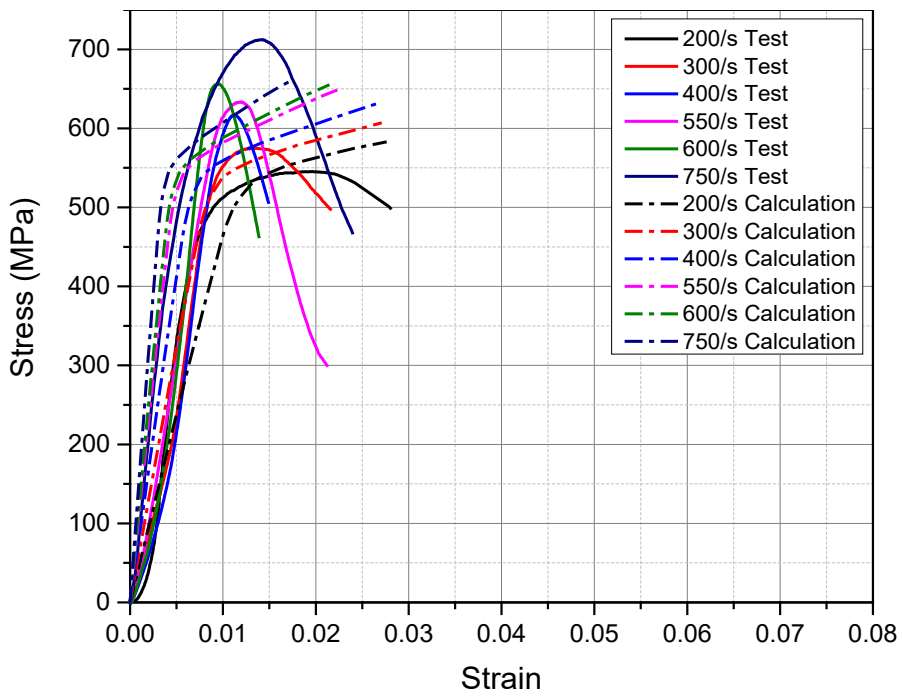

(a) X direction

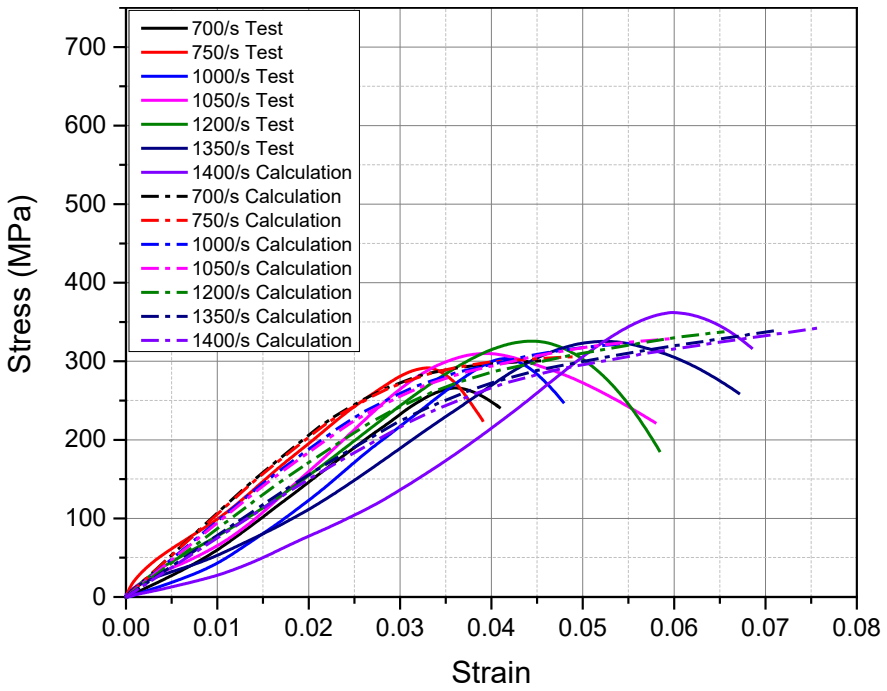

(b) Y direction

Figure 7. Stress–strain curve of LAM-02 at different strain rates under dynamic compression

As shown in Figure 7, both along the X and Y directions, the LAM-02 laminate exhibited nonlinear characteristics in the initial stage, and then was linear. But when near to the failure point, the material exhibited nonlinear features again, similar to the results of the static tests. It showed an obvious strain rate hardening effect along both directions, and the strength of dynamic compression was significantly higher than that of static loading: along the X direction, the strength was approximately 20% higher, whereas it was 40% higher along the Y direction. Moreover, the compressive strength increased with the increase in the strain rate. By comparing the experimental results with the theoretical results, we found that the theoretical predictions of strength and yield limit were more accurate but the theoretical failure strain had a larger error. These conclusions are consistent with those of the previous section. Further, the difference between theoretical calculations and experimental results along the Y direction was greater than that along the X direction, and was mainly expressed in the predicted failure strain.

In addition to the above, we found from the test data that part of the specimens was broken both under high and low strain rates, and the failure stresses were almost identical. This phenomenon was caused by the varying conditions during the processing, hot-pressing, and curing of the CFRP material, where the difference was due to internal damage. Because of the laminated structure of the CFRP composite material, interlaminar adhesive force was relatively low. The delamination generated during the loading process can also affect the performance of the material. The curing and pressing processes of the CFRP material were

unable to achieve an exact duplicate, and the experimental conditions had some influence. Thus, an inevitable dispersion existed in the dynamic compressive failure data of the CFRP material, and was more obvious in the initial processing defects under dynamic loading than under static loading, which also is a difficult problem to tackle to study the dynamical mechanical properties of CFRP materials [30-31].

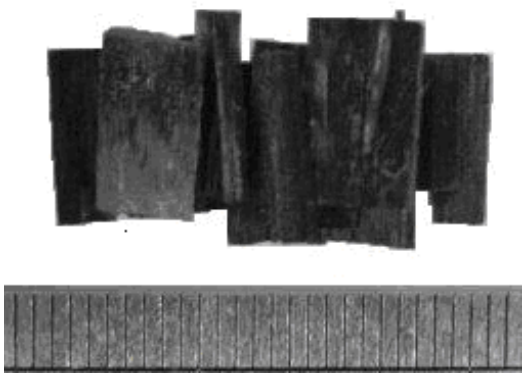

(a) X direction

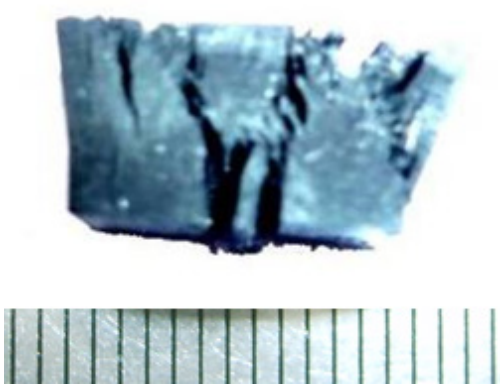

(b) Y direction

Figure 8. The failure mode of CFRP along the X and Y directions under dynamic compression.

The dynamic compression failure mode of CFRP was shown in Figure 8. Along the X direction, the dynamic failure mode of the specimen was identical to the static failure mode, which was mainly delamination accompanied by the breakage and pull-out of the fiber, and fiber matrix debonding. But under dynamic loading, the degree of damage was greater, the delamination was more obvious, and the damage was more typical with the increase in the strain rate. The reasons of this phenomenon are as follows: First, when the strain rate was

high, because of the transverse inertial effect of the fiber, the buckling deformation velocity was lower than the dynamic loading velocity, such that the anti-buckling capacity of the fiber under high deformation led to an increase in compressive strength. Second, the mechanical properties of the fiber and matrix were not uniform, and the stress wave was thus propagated back and forth, resulting in a region of shear stress or tensile stress at the fiber–matrix interface or the interlaminar interface, which caused delamination failure. The failure mode of the specimen along the Y direction was still dominated by the shear failure of the fiber and matrix. In addition to two clear shear cracks at 60°, there was a large longitudinal split and some small cracks. It was evident that the fiber and matrix exhibited the debonding phenomenon in the cracks. With the increase in the strain rate, the failure mode was more severe.

In summary, compared with the failure mode of the specimen subjected to static load, that along X and Y directions under dynamic loading was similar, but was more obvious and intense. It also had a certain correlation with the strain rate.

Because the experimental results did not contain some more details—except for the surface in-plane strain and ultimate failure state—and the calculation program based on bridging model obtained the sequence of damage to each layer, the corresponding stress in the fiber and matrix, and the results of other progressive strength calculations results, the progressive failure phenomena of the laminated structure could be analyzed based on the results of theoretical calculations. The mechanical characteristics related to fiber breakage and matrix damage of the composite material were analyzed.

The progressive failure phenomena of the LAM-02 laminate with compression along the X and Y directions at a strain rate of 750 /s is discussed, the failure sequence of each layer is shown in Figure 9, and the corresponding principal stresses in the fiber and matrix are shown in Figure 10

As shown in Figures 9 and 10, comparing the failure sequence and the corresponding principal stress in the fiber and matrix with the ply orientation of each layer, we found that for the laminate subjected to compression along the X direction compression, the first 23 failed layers were all 0° plies, and the failure mode was fiber breakage. The 90° plies were the last to fail and the failure mode was matrix damage. The failure mode of all 0° and ±45° plies was fiber breakage. For the laminate subjected to compression along the Y direction, the first four failed plies were at 90°, and the failure mode of these was fiber breakage. All plies at 90° and ±45° failed owing to fiber breakage, whereas the 0° plies failed due to matrix damage. These phenomena obtained because for the laminate subjected to load along the X direction, the smaller the angle between the fiber and the axis, the more obvious the strengthening effect of the fiber on the matrix. With increase in the angle of the fiber, the CFRP material performed more like the matrix; therefore, failure mode of the 0° and ±45° plies was fiber breakage, and that of the 90° plies was matrix damage. The opposite phenomena along the Y direction occurred because the larger the angle between the fiber and the Y-axis, the smaller the angle between the fiber and the X-axis. Thus, the performance was the converse of that along the X direction. This phenomenon has been proven by Kawai [32].

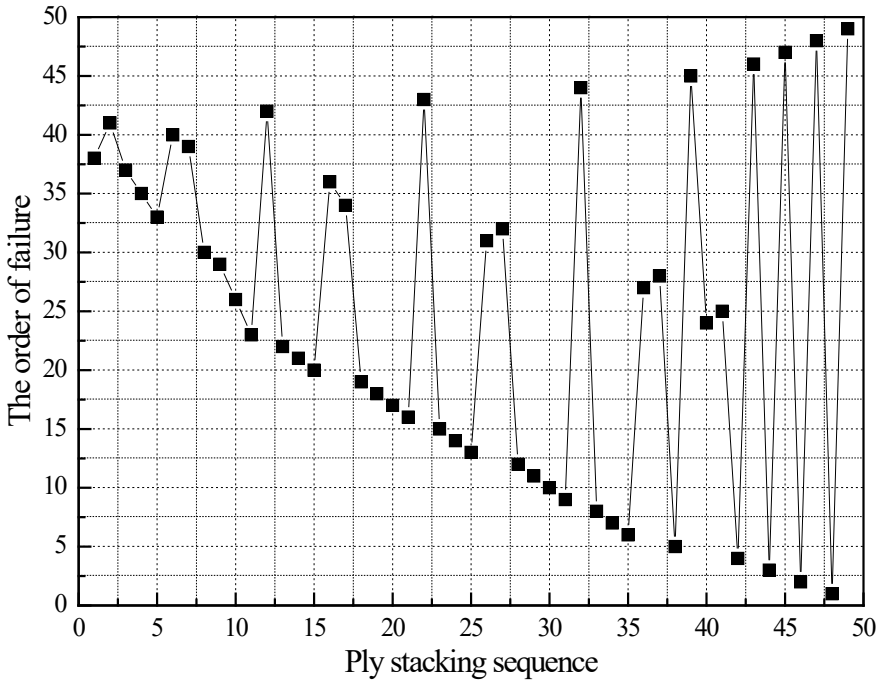

(a) X direction

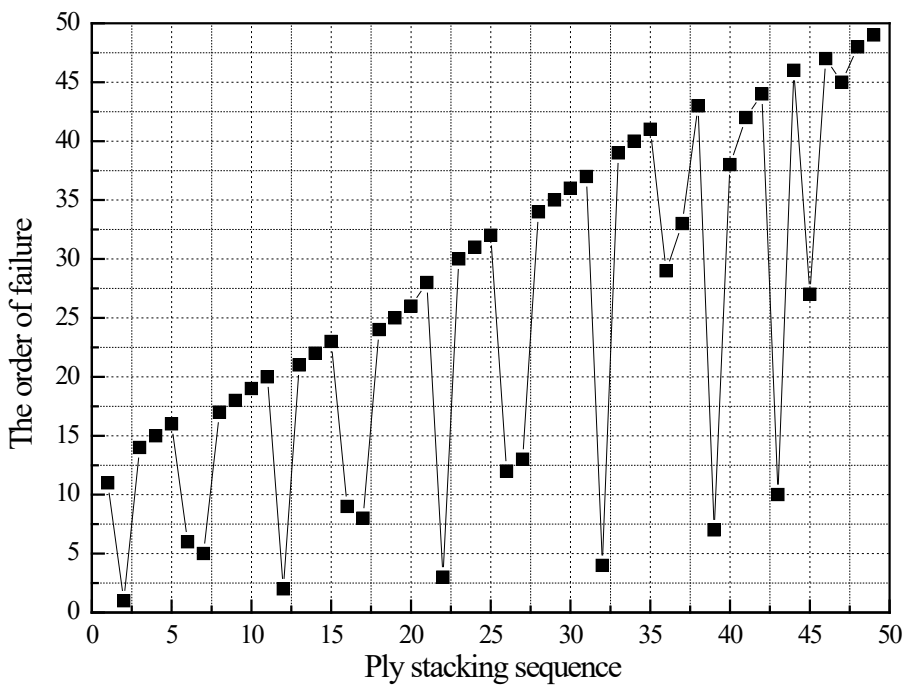

(b) Y direction

Figure 9. The order of failure of laminate along the X and Y directions under compression when the strain rate was 750 /s.

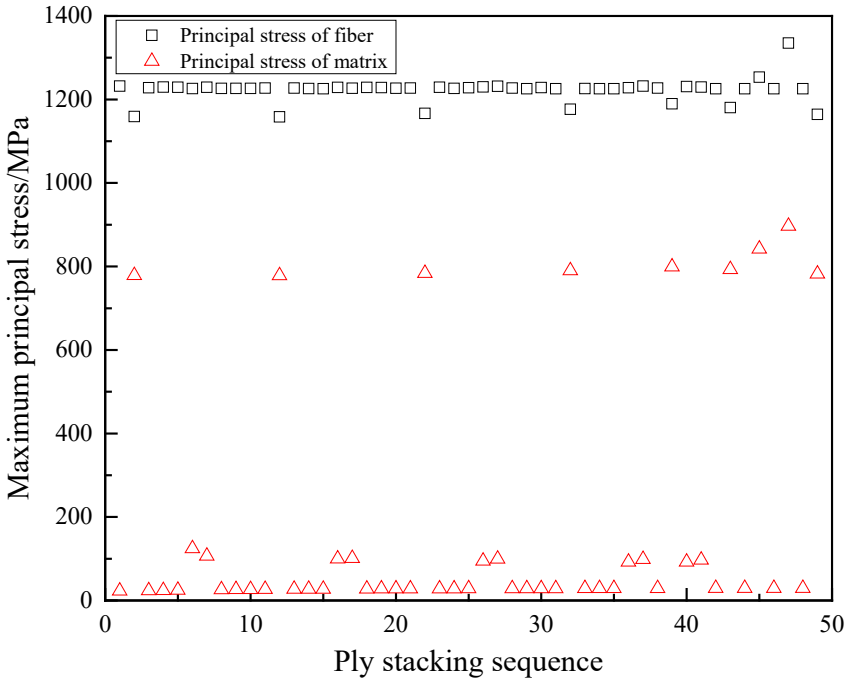

(a) X direction

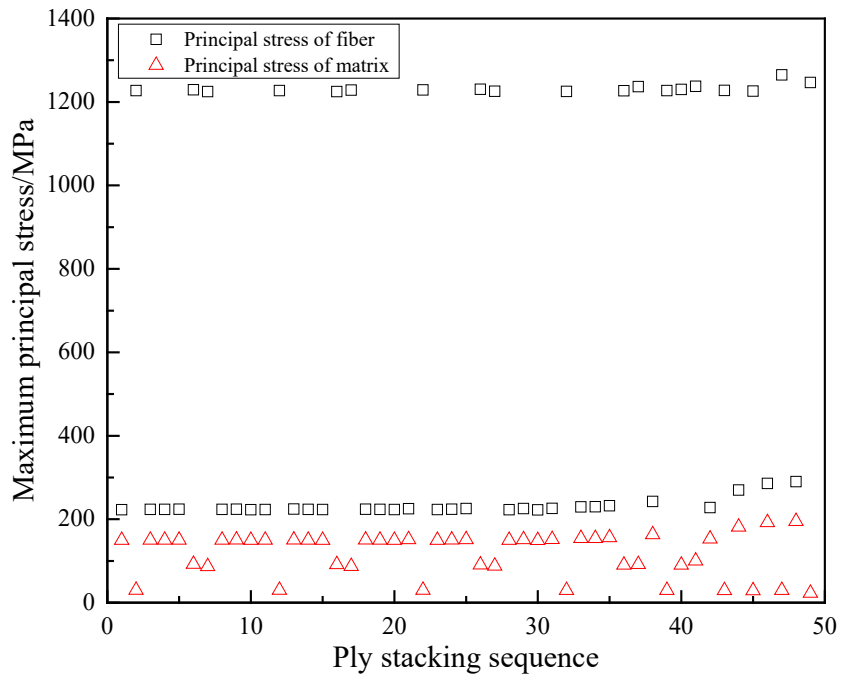

(b) Y direction

Figure 10. The maximum principal stress of fiber and matrix when the laminate failed.

4. CONCLUSION

In this study, theoretical and experimental work is carried out concerning the design requirements of a CFRP laminated structure used for penetrator case under a high-impact load. Considering the strain rate effect, adaptability modification was first conducted for the bridging model, and some test results were used for the verification and validation of the modified model. The theoretical results agreed well with the experimental results. On the basis of this, several structural design schemes of anti-high-impact load CFRP laminate were analyzed, and a new type of laminate satisfying the operating requirements was selected and prepared. Experiments involving quasi-static and medium strain rate compressions were carried out, where the results of our theoretical calculation agreed with the test results. Moreover, the progressive failure phenomena of the laminate structure was discussed by using the calculation program. The main conclusions are as follows:

(1) The constitutive model of rate dependence and failure criterion were combined with the bridging model, and this can be effectively used to analyze the mechanical behavior of CFRP laminates under static and dynamic loads.

(2) The micromechanical characteristics during the failure of the laminate structure were given using strength calculation theory based on the bridging model. The progressive failure phenomena, the mechanical characteristics of the failure mode, and other details of the failure were analyzed.

(3) Based on optimization analysis, the CFRP laminate satisfied the performance requirements, and a series of SHPB experiments on its dynamic mechanical properties were conducted. The specimens all exhibited strain rate dependence along the X and Y directions, and this characteristic was reflected by the improved bridging model. The delamination phenomenon of under in-plane load condition led to lower compressive strength than in the theoretical prediction.

REFERENCES

[1] Thiruppukuzhi SV, Sun CT. Testing and modeling high strain rate behavior of polymer composites. Composites Part B. 1998 Sept; 29(5): 535-546.

[2] Jadhav A, Woldesenbet E, Pang SS. High strain rate properties of balanced angle-ply graphite/epoxy composites. Composites Part B. 2003 Jun; 34(4): 339-436.

[3] Ochola RO, Marcus K, Nurick GN, Franz T. Mechanical behaviour of glass and carbon fibre reinforced composites at varying strain rates. Compos Struct. 2004. 63(3-4): 455-467.

[4] Naik N K, Kavala VR. High strain rate behavior of woven fabric composites under compressive loading. Mater. Sci. Eng., A. 2008 Feb; 474(1-2): 301-311.

[5] Kara A, Tasdemirci A, Guden M. Modeling quasi-static and high strain rate deformation and failure behavior of a (+/- 45) symmetric E-glass/polyester composite under compressive loading. Mater Design. 2013 Aug; 49: 566-574.

[6] Huang ZM. An introduction to micromechanics of composites. Science Press; 2004 (in Chinese).

[7] Hopkins DA, Chamis CC. A unique set of micromechanics equations for high temperature metal matrix composites. NASA TM 87154, 1985.

[8] Chamis CC. Mechanics of composite materials: Past, present and future. Comp Technol Res ASTM. 1989; 11(1): 3-14.

[9] Hill R. Theory of mechanical properties of fiber-strengthened materials. J. Math. Phys. 1964; 12(12): 199-212.

[10] Hill R. A self-consistent mechanics of composite materials. J Mech Phys Solids. 1965 Aug; 13(4): 213-222.

[11] Hashin Z, Rosen BW. The elastic moduli of fiber-reinforced materials. J Appl Mech. 1964 Jun; 31(2): 223-232.

[12] Hashin Z. On elastic behavior of fiber-reinforced materials. J Mech Phys Solids. 1965; 13(3): 119-134.

[13] Huang ZM. Micromechanical prediction of ultimate strength of transversely isotropic fibrous composites. Int J Solids Struct. 2001 May-Jun; 38(22-23): 4147-4172.

[14] Huang ZM. Simulation of the mechanical properties of fibrous composites by the bridging micromechanics model. Composites Part A. 2001 Feb; 32(2): 143-172.

[15] Zhang HS, Huang ZM. A micromechanics model for predicting strengths in fiber laminated composites plate under low-velocity impact. Fiber Reinforced Plastics/Composites, 2008 (5): 12-17 (in Chinese).

[16] Shokrieh MM, Ornidi MJ, Mosalmani R. Strain-rate dependent micromechanical method to investigate the strength properties of glass/epoxy composites. Compos Struct. 2014 May; 111(11): 232-239.

[17] Shokrieh MM, Mosalmani R, Ornidi MJ. A strain-rate dependent micromechanical constitutive model for glass/epoxy composites. Compos Struct. 2015 Mar; 121:37-45.

[18] Huang ZM. Latest advancement of the bridging model theory. Appl Math Mech. 2015, 6(36): 563-581 (in Chinese).

[19] Grudza ME, Flis WJ, Lam HL, Jann DC, Ciccarelli RD. Reactive Material Structures. DE TECHNOLOGIES INC KING OF PRUSSIA PA; 2014 Mar 31.

[20] Chen W, Zhou B. Constitutive behavior of Epon 828/T-403 at various strain rates. Mech Time-Depend Mat. 1998; 2(2): 103-111.

[21] Gilat A, Goldberg RK, Roberts GD. Experimental study of strain-rate-dependent behavior of carbon/epoxy composite. Compos Sci and Technol. 2002 Aug; 62(10-11): 1469-1476.

[22] Xiaoping H, Shengliang H, Hua L. Study of constitutive mode and dynamic mechanical properties of composites at different temperatures. Mech Sci Technol. 1999; 1: 125-126 (in Chinese).

[23] Zhou Y, Xia Y. In situ strength distribution of carbon fibers in unidirectional metal-matrix composites-wires. J. Compos Sci and Technol, 2001 Nov; 61(14): 2017-2023.

[24] Karim MR. Constitutive modeling and failure criteria of carbon-fiber reinforced polymers under high strain rate. [Dissertation for the degree of doctor of philosophy], USA: University of Akron, 2005.

[25] Alves M. Material Constitutive Law for Large Strains and Strain Rates. J Eng Mech-ASCE. 2000 Feb; 126(2): 215-218.

[26] Hosur MV, Alexander J, Vaidya UK, Jeelani S. High strain rate compression response of carbon/epoxy laminate composites. Compos Struct. 2001 May-Jun; 52(3-4): 405-417(13).

[27] Guedes RM, de Moura M, Ferreira FJ. Failure analysis of quasi-isotropic CFRP laminates under high strain rate compression loading. Compos Struct. 2008 Aug; 84(4): 362-368.

[28] De Moura M, Marques AT. Prediction of low velocity impact damage in carbon–epoxy laminates. Composites Part A. 2002 Mar; 33(3): 361-368.

[29] De Moura M, Gonçalves JPM. Modelling the interaction between matrix cracking and delamination in carbon–epoxy laminates under low velocity impact. Compos Sci Technol. 2004 Jun; 64(7-8): 1021-1027.

[30] Summerscales J. Manufacturing defects in fibre-reinforced plastics composites. Insight. 1994; 36(12): 936-942.

[31] Advani SG, Sozer EM, Jr LM. Process modeling in composites manufacturing. Assembly Autom. 2002; 56(3): B69-B70.

[32] Kawai M. Saito S. Off-axis strength differential effects in unidirectional carbon/epoxy laminates at different strain rates and predictions of associated failure envelopes. Composites Part A. 2009 Oct; 40(10): 1632-1649.